

Deformation at depth associated with the 12 May 2008 MW 7.9 Wenchuan earthquake from seismic ambient noise monitoring

B. Froment,^{1,2} M. Campillo,¹ J.H. Chen,³ and Q.Y. Liu³

Received 12 October 2012; revised 5 December 2012; accepted 5 December 2012; published 16 January 2013.

[1] We track the temporal evolution of seismic wave speed to detect changes in material properties at depth, driven by deformation associated with the 2008 Mw 7.9 Wenchuan earthquake. We analyze ambient noise correlation functions to monitor seismic wave speed variations. The data were continuously recorded during 2 years by 114 broadband stations in a region that covers the southern two thirds of the ruptured fault. We perform the analysis in the 12-to-20-s period band. By comparison with measurements in the band 1-to-3 s, we show that the seismic velocity changes cannot be explained by a shallow perturbation but are related to deformation at depth in the crust. The spatial and temporal characteristics of these variations can thus be viewed as reflecting the middle crust behavior. In particular, the results suggest that the deformation in the middle crust is different beneath Tibet and the Sichuan basin. **Citation:** Froment B., M. Campillo, J. H. Chen, and Q. Y. Liu, (2013), Deformation at depth associated with the 12 May 2008 MW 7.9 Wenchuan earthquake from seismic ambient noise monitoring, *Geophys. Res. Lett.*, 40, 78–82, doi:10.1029/2012GL053995.

1. Introduction

[2] Investigating the deformation processes occurring in the deep crust is a key issue for developing a comprehensive model of the seismic cycle in continental areas. In the Tibetan region, this becomes even more relevant since large-scale deformation mechanisms are still widely debated. In particular, questioning about the formation of the Longmen Shan, which constitutes the eastern margin of the Tibetan plateau, has led to two main contradictory models for deformation in the area: a *rigid block model* in which the deformation is explained by crustal faulting and shortening [e.g., *Tapponnier et al.*, 2001] and a *channel flow model*, which is based on ductile deformation of the deep crust beneath the Tibetan plateau in a weak (low viscosity) layer [e.g., *Royden et al.*, 1997; *Clark and Royden*, 2000; *Burchfiel et al.*, 2008]. An important distinction between these two competing models

lies in the nature of deformation in the deep crust (i.e., ductile versus brittle). In this context, we propose to use the response of the crust after the major Wenchuan earthquake to provide insights into deformation processes at depth in this region.

[3] On 12 May 2008, the M_w 7.9 Wenchuan earthquake caused more than 80,000 fatalities, as well as widespread catastrophic damage in the Sichuan province of China. The Wenchuan quake is one of the largest continental thrust events in the world and took place within the Longmen Shan mountain range that showed limited seismic activity before this event. In October 2006, the Institute of Geology of the China Earthquake Administration deployed almost 300 broadband stations in western Sichuan province. In the present study, we use data from the northern half of this array, which covered two thirds of the fault system that was activated during the Wenchuan earthquake. This Western Sichuan Seismic Array (WSSA) was operational for more than 2 years and provides unique continuous recordings from before, during, and after the Wenchuan quake. The study of such a major earthquake through this very large dataset (both in time and space) therefore presents a unique opportunity to examine crustal deformation at different stages of the seismic cycle.

2. Method and Data

[4] The deformation of the deep crust is poorly resolved by surface geodetic measurements. Seismology is then particularly useful since it gives information about material properties at depth and can thus provide insights into deep processes. In this study, we track the temporal evolution of the seismic wave speed at depth to detect changes in crustal material properties driven by deformation. We use the >2-year continuous recordings to compute seismic ambient noise cross-correlation functions. These correlation functions are used to recover the Green's function between pairs of stations [e.g., *Shapiro and Campillo*, 2004; *Sabra et al.*, 2005] at different dates around the Wenchuan earthquake. The temporal evolution of the crust is then tracked by measuring the seismic wave speed changes between the correlation functions corresponding to different dates [e.g., *Sens-Schönfelder and Wegler*, 2006; *Wegler and Sens-Schönfelder*, 2007; *Brenguier et al.*, 2008a; *Brenguier et al.*, 2008b].

[5] We use the seismic noise recorded by 114 stations located in the fault region (Figure 1a) from 1 January 2007 to the end of 2008. Stations with instrumental timing errors have been removed using a time symmetry argument for noise cross-correlations as introduced by *Stehly et al.* [2007]. Direct waves reconstructed in the correlation functions are highly sensitive to the azimuthal distribution of the noise intensity [e.g., *Froment et al.*, 2010]. We thus restrict velocity change measurements to coda waves (see Supporting Information)

All Supporting Information may be found in the online version of this article.

¹ISTerre, Université de Grenoble 1, CNRS, Grenoble, France.

²Now at the Department of Earth, Atmospheric and Planetary Sciences, Massachusetts Institute of Technology, Cambridge, Massachusetts, USA.

³State Key Laboratory of Earthquake Dynamics, Institute of Geology, China Earthquake Administration, Beijing, China.

Corresponding author: B. Froment, Department of Earth Atmospheric and Planetary Sciences, 54-511, Massachusetts Institute of Technology, 77 Massachusetts Avenue, Cambridge, MA 02139-4307, USA. (fromentb@mit.edu)

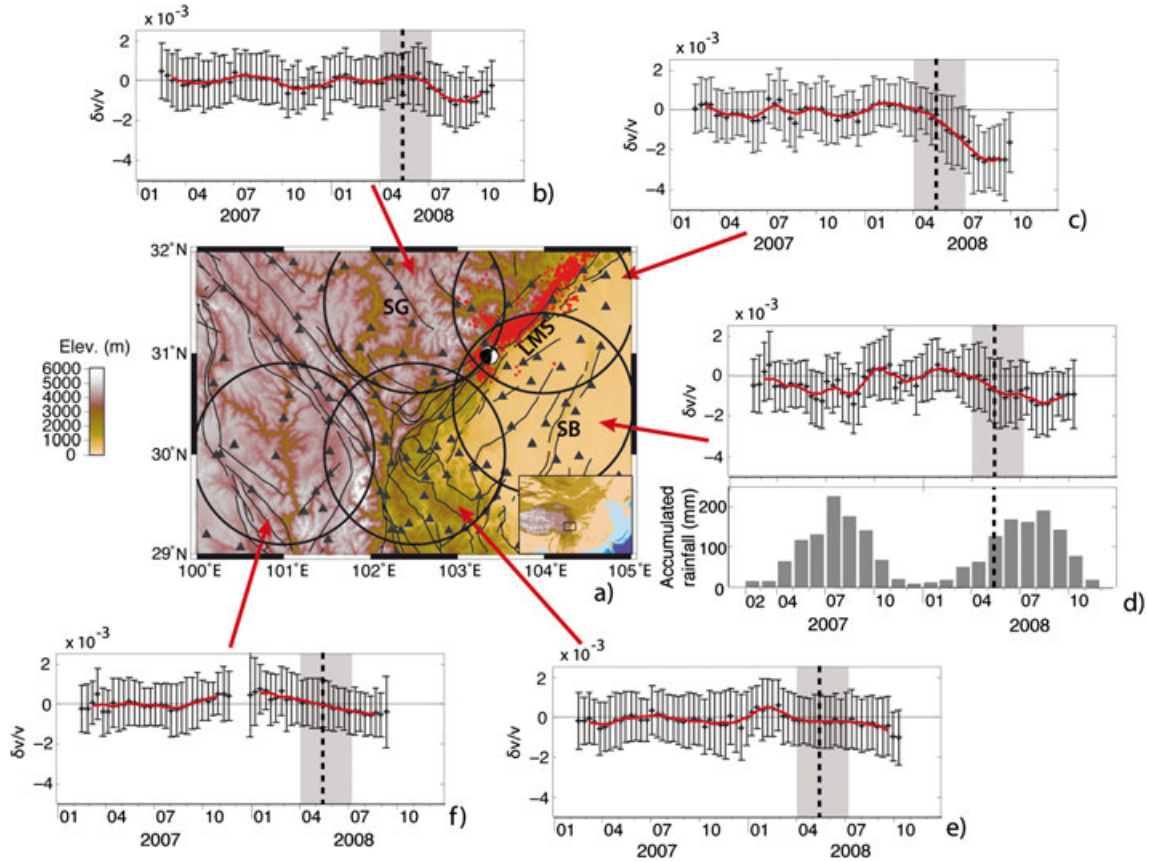


Figure 1. (a) Location map of the stations used in the present study (gray triangles). The beach ball indicates the epicenter of the Wenchuan earthquake, and the red dots represent the aftershocks [Chen *et al.*, 2009]. The black lines show the major faults in the region. SB, SG, and LMS indicate the main geological units to which this study refers, that is, the Sichuan sedimentary basin, the Songpan-Ganzi block, and the Longmen Shan fault zone, respectively. Finally, the black circles indicate the limits of five 100-km-radius sub-regions considered in this study. (b–f) The temporal seismic velocity changes in each sub-region. The crosses and error bars correspond, respectively, to the average and standard deviation of the measurements done at each date on the different station pairs that fall into each sub-region. Only measurements with a correlation coefficient higher than 0.9 are considered (see text for explanation). Red curves show the trend of the temporal evolution by averaging measurements (crosses) over five dates. The vertical dashed line in each figure shows the date of the Wenchuan earthquake, and the gray shadow zone around this illustrates the 100-day stack window. Finally, Figure 1d shows also the monthly accumulated rainfall in the entire region for the 2-year period.

to mitigate the effects of temporal variations in the distribution of the noise sources.

[6] Assuming the diffusion approximation for seismic coda waves, the equipartition principle implies that surface waves dominate the seismic coda [e.g., Margerin *et al.*, 2009]. Therefore, our coda-based measurements can be considered as surface-wave-based measurements, which leads to a relationship between the period band considered and the depth investigated: longer periods are sensitive to deeper structures. To study the behavior of the deep crust, we thus focus on velocity changes for relatively long periods. However, the longer the periods, the more difficult the noise-based velocity change measurements are technically. This is partly due to weaker scattering at long periods which limits the duration of the meaningful coda. We have therefore restricted our analysis to periods less than 20s and consider the 12-to-20-s period band centered on the primary microseismic noise peak. In the region of interest, this frequency band is mostly sensitive to the middle crust (maximum sensitivity for ~10–20km depth; see

Figure 2). Moreover, the longer the periods, the slower the convergence of the noise correlations toward the Green’s function is [e.g., Larose *et al.*, 2007]. This slow convergence is another difficulty in the consideration of long-period signals. We thus need to consider 100-day stacked noise correlation functions which will limit the temporal resolution of our results. For each station pair, we then track the temporal variations by comparing the stacked correlation function at each date, to a reference correlation function that is the average over the whole 2-year period. The seismic velocity variations are computed by the so-called *stretching* method [e.g., Lobkis and Weaver, 2003; Sens-Schönfelder and Wegler, 2006] (see Supporting Information for processing details).

[7] The relatively large scale of the study region allows us to investigate the temporal seismic velocity changes in different sub-arrays. In practice, this regionalization corresponds to averaging the velocity change measurements over station pairs that fall into 100-km-radius sub-regions. To consider only the reliable measurements, we select the

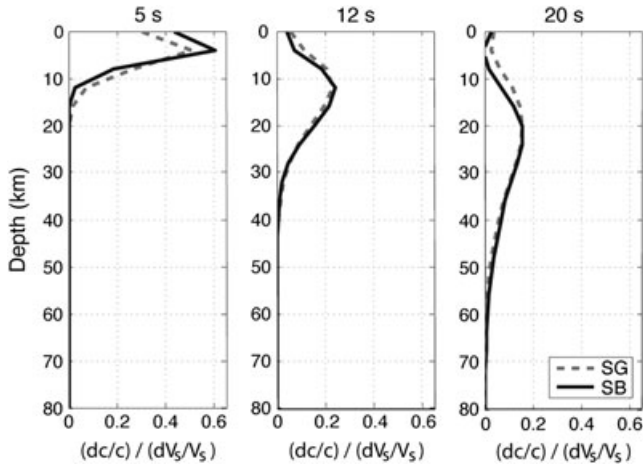


Figure 2. Sensitivity of the Rayleigh phase velocity c , to a shear velocity perturbation dV_s . A perturbation in a 4-km-thick layer is considered, and the sensitivity of c to this perturbation is computed as a function of the depth of the perturbed layer (Huang and Van der Hilst, personal communication, 2010). The sensitivity analysis was carried out: (1) for different periods, as 5 s (left), 12 s (middle), and 20 s (right); and (2) considering velocity models for both sides of the Longmen Shan fault zone, that is, the Songpan-Ganzi block (gray dashed line) and the Sichuan basin (black line). Note that we consider Rayleigh waves since they are supposed to dominate the coda of the vertical-vertical correlation functions used in this study [Margerin *et al.*, 2009].

data that correspond to a good correlation (>0.9) between the current correlation function and the reference. This correlation coefficient quantifies the resemblance between the two correlation functions once the velocity change effects have been corrected by the stretching technique, and therefore, it can be viewed as a quality criterium of the velocity change estimation.

3. Results

[8] Figure 1 synthesizes the temporal relative seismic velocity changes for five sub-regions.

[9] We observe a clear seismic velocity drop after the Wenchuan earthquake around the fault zone where the aftershocks were distributed and the rupture propagated (Figure 1c).

[10] For the Songpan-Ganzi area (Figure 1b), we identify a smaller velocity drop after the main shock. Although the error bars do not fall below zero, we note that the amplitude of the drop is larger than the temporal fluctuations in the period preceding the event. The results from the other side of the rupture zone, that is, in the Sichuan basin sub-region (Figure 1d), are less clear. We observe a velocity drop after the time of the earthquake, but Figure 1d shows also some variations during summer 2007. They could be the mark of a seasonal long-term trend also visible after the Wenchuan earthquake. The actual amplitude of a potential velocity change associated with the earthquake is therefore difficult to assess. Finally, the medium seems quite stable along the 2-year period in the southern part of the region (Figures 1e and 1f). Note that the 100-day stack (illustrated by the gray

shadow zones in Figure 1) induces a temporal smoothing in the $\delta v/v(t)$ measurements.

[11] Figure 1c shows a velocity drop that reaches $>0.2\%$. In comparison, the seismic velocity drop observed at shorter periods (between 1 s and 3 s) is less than 0.1% (see Figure 3 and *Chen et al.*, [2010]). According to the sensitivity shown in Figure 2, a shallow perturbation cannot explain larger measured velocity changes at longer rather than at shorter periods. This observation is particularly relevant since physical mechanisms that cause seismic velocity variations associated with earthquakes remain under debate. In particular, it is often discussed whether these variations are associated with the response of superficial soil layers to strong shaking or with static stress changes and deformation at depth.

[12] This amplitude argument allows us to consider that the seismic velocity variations observed in Figure 1 are representative of a perturbation extending at depths larger than the penetration of the short period waves. According to Figure 2, our measurements have their stronger sensitivities between 10 and 20 km. They therefore likely reflect the deformation in the intermediate crust around the Wenchuan earthquake.

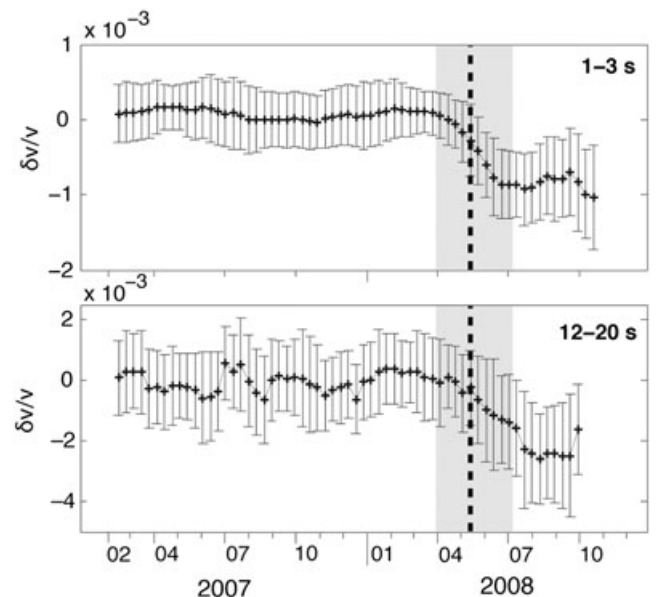


Figure 3. Comparison of the temporal seismic velocity changes in the LMS sub-region (see Figure 1a) measured in two different period bands: between 1 s and 3 s (top) and between 12 s and 20 s (bottom). Note that the bottom figure corresponds to the measurements shown in Figure 1c. The crosses and error bars correspond, respectively, to the average and standard deviation of the series of measurements on the different station pairs at each date. The vertical dashed line shows the date of the Wenchuan earthquake, and the gray shadow zone around this illustrates the 100-day stack window. Note the different vertical scales in the two figures. As discussed in the text, shorter periods converge faster toward the Green's function and the analysis could thus be done using a shorter stack window (30 days in *Chen et al.*, [2010]). For the sake of simplicity, we compare here measurements in the two period bands using the same 100-day stack duration.

4. Inferences about the Deformation at Depth

4.1. Different Behaviors on Both Sides of the Longmen Shan

[13] The spatial and temporal characteristics of these variations can thus be viewed as reflecting the middle crust behavior around the Wenchuan earthquake. Figures 1b and 1d show a different behavior on both sides of the fault, with an apparent seasonal trend beneath the Sichuan basin well correlated with the rainfall in the region (Figure 1d). This trend is not visible beneath the Tibetan plateau, where the only seismic velocity drop is observed after the Wenchuan earthquake.

[14] Note that in view of the amplitude of these seasonal fluctuations and the measurement uncertainties, they must be discussed cautiously. The difference between these two areas makes us suggest that the seismic velocity variations measured beneath the thick (>10km) sedimentary Sichuan basin could be influenced by an external seasonal process. The hypothesis that this seasonal pattern is an artefact due to variations in noise source location [e.g., *Stehly et al.*, 2006; *Landès et al.*, 2010; *Froment et al.*, 2010] is unlikely for two reasons. First, because we measure velocity variations on coda waves that are expected to be less affected by changes in seismic ambient noise sources. Second, at the periods considered, the noise sources are produced by swell in distant oceans [e.g., *Gutenberg*, 1951; *Stehly et al.*, 2006]. The sources involved, and their effects on velocity change measurements, are thus likely to be similar from the Sichuan basin to the Songpan-Ganzi block. By contrast, this specific signature could reflect the response of the thick sedimentary basin to strain at depth induced by a seasonal surface process, such as changes in surface temperature or rainfall. Note that the seasonal pattern observed here cannot be trivially related to changes in surface temperature or water table that affect directly only very superficial parts of the crust, since it is not observed at short periods [*Chen et al.*, 2010]. The satellite data from the Gravity Recovery and Climate Experiment (GRACE) allow to evaluate the water loading due to the monsoon and to estimate the induced deformation (Chanard, K., J.-P. Avouac, J. Genrich, and G. Ramillien, Modeling deformation induced by seasonal variations of continental water in the Himalaya region: Sensitivity to Earth elastic structure, submitted to *Earth and Planetary Sciences Letters*, 2012). Applied to our region of interest, this approach leads to an estimation of seasonal normal stress fluctuation at 10 km depth beneath the Sichuan basin, of the order of 10^4 Pa [Chanard and Avouac, personal communication, 2012]. This value can be compared to the static co-seismic stress change induced by the Wenchuan earthquake at a regional scale (Shao and Ji, personal communication, 2010). When considering the rupture obtained by *Ji and Hayes* [2008] and averaging the normal stress at 10km depth in a 100-km extended zone around the fault, we find 1-to- 1.5×10^5 Pa. Note that the change in stress due to the earthquake is indeed smaller in the basin. Comparing these values suggests that the effect of continental water loading at depth is not negligible in comparison to the earthquake and thus could be significant for our measurements.

4.2. Post-Seismic Response

[15] Besides highlighting characteristics of the different structures on both sides of the Longmen Shan, the signature of the middle crust also presents a specific temporal

characteristic since the seismic velocity drop following the earthquake is delayed relative to the time of the main shock (Figure 1). This delay is not due to the temporal smoothing caused by the 100-day stack: a co-seismic velocity drop would present its minimum at the beginning of July 2008 (i.e., the right limit of the shadow zone). In contrast, Figures 1b and 1c correspond to a velocity drop delayed by 1 month (to one and a half months) after the main shock. Note that we do not discuss this delay in the Sichuan basin since some seasonal effects may be added to the earthquake signal, making it equivocal. This delay is not observed in the response of the upper crust as indicated by measurements in the 1-to-3-s period band (Figure 3). These results show that the deformation induced by the earthquake in the middle crust is primarily post-seismic, while the upper crust is characterized by a co-seismic response (Figure 3 and *Chen et al.*, [2010]).

[16] Three main processes are usually mentioned to explain post-seismic deformation: (1) visco-elastic relaxation of the deep crust, (2) poro-elastic relaxation in the upper brittle crust, or (3) post-seismic slip. To explain the post-seismic signal observed corresponding to a change at depth, we favor visco-elastic and post-seismic slip hypotheses. The characteristic time in our post-seismic signal is ~ 1 – 1.5 months. This is much shorter than the one deduced by *Ryder et al.* [2011] from the geodetic observations following the Kokoxili earthquake, a strike slip event which occurred in Tibet with a magnitude similar to the Wenchuan event. These authors proposed a visco-elastic process with a viscosity of the crust of about 10^{18} – 10^{19} Pa·s to explain their post-seismic observations. Our observations would require much smaller viscosity values. *Royden et al.* [2008] proposed values as low as 10^{16} – 10^{17} Pa·s for the deep part of the crust beneath the Tibetan plateau, suggested weak by low velocity layers revealed by tomography and receiver function analysis [e.g., *Yao et al.*, 2006; *Yao et al.*, 2008; *Xu et al.*, 2007]. However, the tomographic study by *Li et al.* [2010] suggested that the 12-to-20-s period band is mostly sensitive to layers located above the weak deep crust, making these low values of viscosity irrelevant to our measurements. The value of the observed delay is therefore not easily understandable in terms of visco-elastic response, according to evaluation of the viscosity in the region. As for the second hypothesis, since the Wenchuan earthquake occurred on a listric reverse fault system dipping toward the northwest, post-seismic slip would affect preferentially the Songpan-Ganzi block. Again, because of likely seasonal fluctuations in the Sichuan basin, it is difficult to demonstrate an asymmetric behavior and therefore to unambiguously support the hypothesis of post-seismic slip.

5. Conclusion

[17] This study allows us to examine the spatial and temporal speed changes at depth, which are related to the deformation of the intermediate crust around the Wenchuan earthquake. We have seen that different behaviors show the difference in deformation at depth on both sides of the Longmen Shan. Moreover, this analysis allows us to examine the response of the crust associated with various mechanisms, such as tectonic (during different stages of the seismic cycle) and probable non-tectonic seasonal processes. These results show that noise-based seismic velocity variations constitute an observable that

gives insights into deformation at depth and that appears to be an important tool in the difficult task of investigating deep processes.

[18] **Acknowledgments.** The study was jointly supported by the European Research Council (Advanced Grant Whisper), the Key Projects of Chinese National Programs for Fundamental Research and Development (2004CB418402), and the National Natural Science Foundation of China (40974023). B.F. acknowledges the financial support from Shell Research. Shuncheng Li, Biao Guo, Yu Li, Jun Wang, and Shaohua Qi participated to the acquisition of the field data. We thank Philippe Roux, Diane Rivet, Céline Hadziioannou, Rob van der Hilst, Isabelle Ryder, and Taylor Perron for the helpful discussions, as well as Xavier Briand for the computing support. We also thank the people that kindly provided their results: Guangfu Shao and Chen Ji for the stress changes associated with the Wenchuan earthquake, Kristel Chanard and Jean-Philippe Avouac for the stress variations associated with water loading, and finally Hui Huang and Rob van der Hilst for their sensitivity analysis. We finally thank D. Schaff and an anonymous reviewer who provided helpful comments.

References

- Brenguier, F., N. M. Shapiro, M. Campillo, V. Ferrazzini, Z. Duputel, O. Coutant, and A. Nercessian (2008a), Towards forecasting volcanic eruptions using seismic noise, *Nat. Geosci.*, *1*(2), 126–130, doi:10.1038/ngeo104.
- Brenguier, F., M. Campillo, C. Hadziioannou, N. M. Shapiro, R. M. Nadeau, and E. Larose (2008b), Postseismic relaxation along the San Andreas fault at Parkfield from continuous seismological observations, *Science*, *321*(5895), 1478–1481, doi:10.1126/science.1160943.
- Burchfiel, B. C., et al. (2008), A geological and geophysical context for the Wenchuan earthquake of 12 May 2008, Sichuan, People's Republic of China, *GSA Today*, *18*(7), doi: 10.1130/GSATG18A.1.
- Chen, J. H., B. Froment, Q. Y. Liu, and M. Campillo (2010), Distribution of seismic wave speed changes associated with the 12 May 2008 Mw 7.9 Wenchuan earthquake, *Geophys. Res. Lett.*, *37*, L18,302, doi:10.1029/2010GL044582.
- Chen, J. H., Q. Y. Liu, S. C. Li, B. Guo, Y. Li, J. Wang, and S. H. Qi (2009), Seismotectonic study by relocation of the Wenchuan Ms 8.0 earthquake sequence, *Chinese J. Geophys.-Chinese Ed.*, *52*(2), 390–397.
- Clark, M. K., and L. H. Royden (2000), Topographic ooze: Building the eastern margin of Tibet by lower crustal flow, *Geology*, *28*(8), 703–706, doi:10.1130/0091-7613(2000)28<703:TOBTEM>2.0.CO;2.
- Froment, B., M. Campillo, P. Roux, P. Gouédard, A. Verdel, and R. L. Weaver (2010), Estimation of the effect of nonisotropically distributed energy on the apparent arrival time in correlations, *Geophysics*, *75*(5), SA85–SA93, doi:10.1190/1.3483102.
- Gutenberg, B. (1951), Observations and theory of microseisms, in *Compendium of Meteorology*, edited by T. Malone, pp. 1303–1311, American Meteorological Society, Boston, MA.
- Ji, C., and G. Hayes (2008), Preliminary result of the May 12, 2008 Mw7.9 eastern Sichuan, China earthquake, available on the USGS website <http://earthquake.usgs.gov/eqcenter/eqinthenews/2008/us2008ryan/> (section Scientific and Technical, Finite Fault Model).
- Landès, M., F. Hubans, N. M. Shapiro, A. Paul, and M. Campillo (2010), Origin of deep ocean microseisms by using teleseismic body waves, *J. Geophys. Res.: Solid Earth*, *115*, B05,302, doi:10.1029/2009JB006918.
- Larose, E., P. Roux, and M. Campillo (2007), Reconstruction of Rayleigh-Lamb dispersion spectrum based on noise obtained from an air-jet forcing, *J. Acous. Soc. Am.*, *122*(6), 3437–3444, doi:10.1121/1.2799913.
- Li, Y., et al. (2010), Phase velocity array tomography of Rayleigh waves in western Sichuan from ambient seismic noise, *Chinese J. Geophys.-Chinese Ed.*, *53*(4), 842–852, doi:10.3969/j.issn.0001-5733.2010.04.009.
- Lobkis, O. I., and R. L. Weaver (2003), Coda-wave interferometry in finite solids: recovery of *P*-to-*S* conversion rates in an elastodynamic billiard, *Phys. Rev. Lett.*, *90*, 254,302, doi:10.1103/PhysRevLett.90.254302.
- Margerin, L., M. Campillo, B. A. Van Tiggelen, and R. Hennino (2009), Energy partition of seismic coda waves in layered media: Theory and application to Pinyon Flats Observatory, *Geophys. J. Int.*, *177*(2), 571–585, doi:10.1111/j.1365-246X.2008.04068.x.
- Royden, L. H., B. C. Burchfiel, and R. D. van der Hilst (2008), The geological evolution of the Tibetan plateau, *Science*, *321*(5892), 1054–1058, doi:10.1126/science.1155371.
- Royden, L. H., B. C. Burchfiel, R. W. King, E. Wang, Z. L. Chen, F. Shen, and Y. P. Liu (1997), Surface deformation and lower crustal flow in eastern Tibet, *Science*, *276*(5313), 788–790, doi:10.1126/science.276.5313.788.
- Ryder, I., R. Bürgmann, and F. Pollitz (2011), Lower crustal relaxation beneath the Tibetan Plateau and Qaidam Basin following the 2001 Kokoxili earthquake, *Geophys. J. Int.*, *187*(2), 613–630, doi:10.1111/j.1365-246X.2011.05179.x.
- Sabra, K. G., P. Gerstoft, P. Roux, W. A. Kuperman, and M. C. Fehler (2005), Extracting time-domain Green's function estimates from ambient seismic noise, *Geophys. Res. Lett.*, *32*(3), L03,310, doi:10.1029/2004GL021862.
- Sens-Schönfelder, C., and U. Wegler (2006), Passive image interferometry and seasonal variations of seismic velocities at Merapi Volcano, Indonesia, *Geophys. Res. Lett.*, *33*(21), L21,302, doi:10.1029/2006GL027797.
- Shapiro, N. M., and M. Campillo (2004), Emergence of broadband Rayleigh waves from correlations of the ambient seismic noise, *Geophys. Res. Lett.*, *31*(7), L07,614, doi:10.1029/2004GL019491.
- Stehly, L., M. Campillo, and N. M. Shapiro (2006), A study of the seismic noise from its long-range correlation properties, *J. Geophys. Res.: Solid Earth*, *111*(B10), B10,306, doi:10.1029/2005JB004237.
- Stehly, L., M. Campillo, and N. M. Shapiro (2007), Traveltime measurements from noise correlation: Stability and detection of instrumental time-shifts, *Geophys. J. Int.*, *171*(1), 223–230, doi:10.1111/j.1365-246X.2007.03492.x.
- Tapponnier, P., Z. Xu, F. Roger, B. Meyer, N. Arnaud, G. Wittlinger, and J. Yang (2001), Geology—Oblique stepwise rise and growth of the Tibet plateau, *Science*, *294*(5547), 1671–1677, doi:10.1126/science.105978.
- Wegler, U., and C. Sens-Schönfelder (2007), Fault zone monitoring with passive image interferometry, *Geophys. J. Int.*, *168*(3), 1029–1033, doi:10.1111/j.1365-246X.2006.03284.x.
- Xu, L., S. Rondenay, and R. D. van der Hilst (2007), Structure of the crust beneath the southeastern Tibetan Plateau from teleseismic receiver functions, *Phys. Earth Planet. In.*, *165*(3–4), 176–193, doi:10.1016/j.pepi.2007.09.002.
- Yao, H., R. D. van der Hilst, and M. V. de Hoop (2006), Surface-wave array tomography in SE Tibet from ambient seismic noise and two-station analysis—I. Phase velocity maps, *Geophys. J. Int.*, *166*(2), 732–744, doi:10.1111/j.1365-246X.2006.03028.x.
- Yao, H., C. Beghein, and R. D. van der Hilst (2008), Surface wave array tomography in SE Tibet from ambient seismic noise and two-station analysis—II. Crustal and upper-mantle structure, *Geophys. J. Int.*, *173*(1), 205–219, doi:10.1111/j.1365-246X.2007.03696.x.